



## Electrochemical impedance spectroscopy behavior of aluminum alloys 2024 and 6061 in rainwater

Sahib M. Mahdi, Saraa M. Mohammed

Department of Material Engineering, College of Engineering, Mustansiriyah University, Baghdad, Iraq.

Received 22 April. 2022; Received in revised form 1 July. 2022; Accepted 1 July. 2022; Available online 10 July. 2022

### Abstract

AA2024 and AA6061 solution heat treatable aluminum alloys, which are used in the manufacture of aircraft hulls and structures for their superior mechanical properties. Exposure to a changeable atmosphere, especially rainwater, requires knowledge of the corrosion behavior of these alloys when exposed to rainwater. In the present work the EIS behavior of solution heat-treated and aging of alloys 2024 and 6061 in natural rainwater, were studied before and after solution heat treatment. XRD and SEM detections are used for determining the composition of precipitate particles and the surface morphology after corrosion. The Nyquist curves for the EIS test, agree with equivalent circuits fitting the model of Constant Phase Element (CPE), the polarization resistance ( $R_p$ ), and the capacitance ( $C_f$ ) values recorded for these alloys. The EIS tests show a fluctuation in ( $R_p$ ) and ( $C_f$ ) values and reaction order ( $\alpha$ ) is less than 0.7 clarifying that the surface – rainwater reactions are unequal due to non-uniform sizes and dispersions of precipitation particles ( $Al_2Cu$ ) and ( $Mg_2Si$ ) for both alloys, as well as the coating layer formation of the corrosion products. The corrosion resistance of 2024 is lower than 6061 in rainwater.

*Copyright © 2022 International Energy and Environment Foundation - All rights reserved.*

**Keywords:** Aircraft aluminum alloy; Solution treatment, Electrochemical impedance spectroscopy test, EIS curve.

### 1. Introduction

There are two Al alloy types considered, such as the wrought and cast aluminum alloys [1]. Heat treatment is the process of changing physical and mechanical properties of metal by heating and cooling it while retaining its shape [2]. Solution heat treatment of the aluminum alloys provides the possibility for maximal hardening solute concentration for dissolving into the solution. Such a process is often performed through heating alloy to the temperature where there is a single, solid phase. By performing this process, the atoms of the solute which have been, at first, a portion of a two-phase solid solution are dissolved in solution and produced a single phase. As soon as the alloy is heated to the suggested temperature of solution treatment, it will be quenched at a faster rate in a way that the atoms of the solute have no sufficient time for precipitating out of that solution. Due to the quenching, a supersaturated solution is formed between the Al matrix and the solute [3, 4]. Solution heat treatment was performed to dissolve any relevant alloying elements in a solid [5]. Post held at the treating temperature of the solution for sufficient time for the diffusion of the atoms of solute in the matrix of the solvent to take place, it's quenched to a lower degree of the temperature (for example, room temperature) for keeping the elements of alloying trapped within

the solution. Throughout the aging, the elements of the alloying are trapped in the precipitate of the solution for forming an even distribution of highly fine particles [6]. The material is aged, naturally (at room temperature) or artificially (temperatures usually up to 200°C), for a certain time to get controlled precipitation of strengthening particles[5]. In the case where it has been aged through the re-heating to an intermediate degree of the temperature, it will be designated as the T6 condition (which indicates that the solution is heat-treated and aged artificially) [6]. The goal of the solution heat treatment of Al is obtaining maximal hardening solute concentration, like Zn, Mg, and Cu, in the solution through heating alloy to a degree of the temperature where the single-phase is going to be produced [7, 8]. All non-heat-treatable alloys have a high resistance to general corrosion. Heat-treatable wrought alloys have a significantly lower resistance to general corrosion. These include all 2xxx series alloys (Al-Cu, Al-Cu-Mg, Al-Cu-Si-Mg) in which copper is a major alloying element. As a result of the presence of copper in this type of alloy, the resistance decreases and therefore preventive measures must be taken [9]. The aluminum alloys series 2000 has less corrosion resistance than those alloys that do not contain these elements. For this reason, it is usually difficult to prevent corrosion of aluminum alloys in this series [10]. The 2xxx Al alloys are largely used in the aircraft industry due to their superior mechanical properties resulting from alloying elements addition, mainly Cu and Mg, and precipitation hardening treatments. [11, 12]. Aluminum alloy 6061 is a wrought Al-Mg-Si alloy. It is hardened by heat treatment. Additions of Mg and Si are made to allow the formation of secondary precipitates consisting of Al-Mg<sub>2</sub>Si or Mg<sub>2</sub>Si which form upon heat treatments, thus hardening the aluminum matrix by affecting the mobility of dislocations within the metallic crystals [13, 14]. The 6xxx aluminum alloys combine good mechanical strength and corrosion resistance [15]. As a consequence, they are considered excellent structural materials for a variety of engineering applications in the aerospace and automotive industries [16]. Corrosion in aluminum and its alloys, is usually local and is most commonly caused by pitting or in areas that come into contact with dissimilar minerals in a conducive environment (seawater or road splash containing dissolved salts) [17]. (EIS) it is a distinctly touchy definite technique used for non-destructively evaluating the electrical reaction of chemical structures. EIS systems reflect the chemical system's time reaction using alternating current (AC) voltages of low amplitude over a range of frequencies. Using an electrode setup including an operation, reference, and counter electrodes a known voltage is passed voltage of the counter electrodes is passed through an electrolytic solution from the working electrode and into the counter electrode. Quantitative measurements are provided through the EIS and allow the evaluation at the electrode interface and in the electrolytic solution of small-scale chemical mechanisms. Therefore, in the study of batteries, corrosion, and so on, EIS is useful in evaluating a wide variety of dielectric and electrical characteristics of components [18].

## 2. Experimental procedure:

### 2.1 Aluminum alloys

The materials used in this study are aircraft aluminum alloys of a certain grade (2024 and 6061). The chemical compositions of these alloys were analyzed with spectromax, and the results are reported in Table 1. The results were found to be consistent with the standard values [19]. This study was carried out in natural rainwater. The plate was cut using a water jet to match the dimensions of the sample holder. The disc-shaped specimens are ( $\phi 25 \times 2$  mm) in size.

Table 1. Chemical analysis of the aircraft aluminum alloys.

Element	% Si	Fe	Cu	Mn	Mg	Cr	Ni	Ti	Zn	Pb	Al
AA2024	0.0501	0.178	4.70	0.515	1.46	0.0082	0.0093	0.0240	0.209	0.0073	92.8
AA6061	0.596	0.533	0.257	0.124	0.990	0.121	0.0098	0.132	0.0269	0.0124	97.2

### 2.2 Water media

Natural rainwater was used as a corrosive medium in this study to evaluate solution heat treatment affecting corrosion behavior of both 2024 and 6061 aircraft aluminum alloys at room temperature (25°C). The chemical analysis of rainwater media is shown in Table 2.

### 2.3 Solution Heat treatment

Both 2024 and 6061 aircraft aluminum alloys were treated with a solution heat treatment. The samples were heated in the lab furnace at 530°C for AA 6061 and 495°C for AA 2024 both for 2 hours, then

quenched in distilled water. Both alloys are aged for 1 and 2 hours at temperatures 150, 200, 250, and 300°C.

Table 2. Chemical analysis of natural Rain Water.

Type of analysis	pH	EC ( $\mu\text{s}/\text{Cm}$ )	T.D.S. (mg/l)	$\text{Ca}^{+2}$ (mg/l)	$\text{Mg}^{+2}$ (mg/l)	$\text{CaCO}_3$ (mg/l)	$\text{Cl}^-$ (mg/l)	$\text{HCO}_3^-$ (mg/l)	$\text{SO}_4^{-2}$ (mg/l)	$\text{NO}_3^-$ (mg/l)	$\text{NO}_2^-$ (mg/l)
percentage	5.7	65.03	37.0	4	4.8	30	1.15	12.75	2.83	0.88	0.003

### 3. Results and discussion

#### 3.1 Electrochemical Impedance Spectroscopy (EIS) before heat treatments in rainwater

EIS test results of AA2024 and AA6061 alloy in rainwater are shown in Figure 1, where Figure 2 shows the Constant Phase Element (CPE) of the equivalent circuit for the curves fitting model. The resistors and capacitor data that had been gained from the Nyquist plots are listed in Table 3. By comparing the polarization resistances ( $R_p$ ) for AA2024 and AA6061 it is clear that, the ( $R_p$ ) of AA2024 alloy is higher than for AA6061 in rainwater. While the solution resistance ( $R_u$ ) for both alloys is reverse in values. The reaction order ( $\alpha$ ) values were about the same. The capacitance ( $C_f$ ) of AA2024 alloy is higher than AA6061, leading to more charge transfer that decreases corrosion resistance of AA2024. The explanation is the AA2024 alloy is more sensitive to rainwater than the AA6061 alloy.

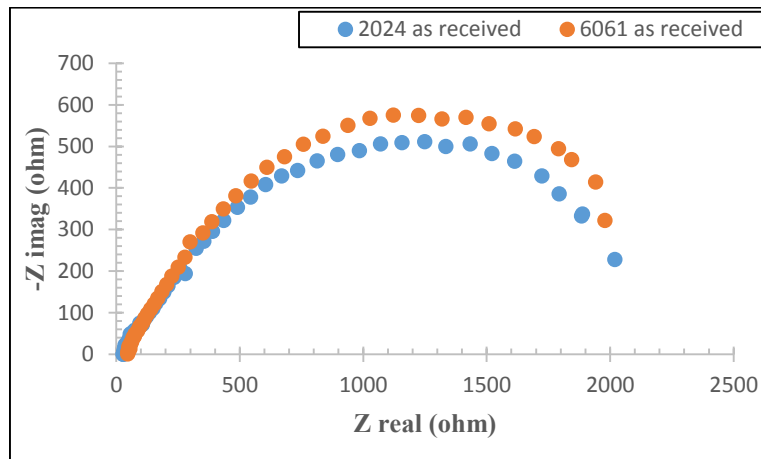


Figure 1. EIS test results of AA2024 and 6061 alloys before solution heat treatment at rainwater.

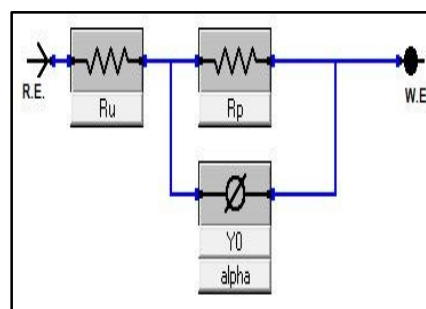


Figure 2. Model of Constant Phase Element (CPE) ( $R_p$ = polarization resistance,  $R_u$ = solution resistance,  $Y_0$ = interface capacitance,  $\alpha$ = order reaction generally 0.9-1.0) ( $\alpha=1$  for an ideal Capacitor).

Table 3. The resistors and capacitors of AA2024 and AA6061 alloy before solution heat treatments in rainwater.

Alloys	$R_p$ ( ohms)	$R_u$ ( ohms)	$C_f(\mu\text{F})$	$\alpha$
AA2024	$2.382 \times 10^3$	22.82	120.2	0.526
AA6061	$2.34 \times 10^3$	41.49	83.03	0.582

Where:  $R_p$ = polarization resistance,  $R_u$ = solution resistance,  $C_f$ = the metal –lectrolyte interface,  $\alpha$  = reaction order.

### 3.2 Effect of solution treatment on electrochemical impedance spectroscopy of 2024 and 6061 aircraft aluminum alloys

The Nyquist curve for EIS test results of AA2024 and AA6061 alloys in rainwater after heat treatment is shown in Figures 3, 4, 5, and 6. Tables 4 and 5 show the resistors, capacitors, and values of reaction order that had been gained from the Nyquist plots by using a CPE fit for both alloys.

Figure 3 shows EIS test results of solution heat treatment of AA2024 alloy that artificially aged at temperatures (150, 200, 250, and 300°C) with aging time 1 hour, and exposed to natural rainwater. From this figure, by comparing the resistances and capacitors, the polarization resistance ( $R_p$ ) for the aging temperatures were varied decreasing and increasing with aging temperatures. This behavior is due to the intermetallic compound precipitation ( $Al_2Cu$ ) its size and distribution on the sample surface. The capacitors ( $Y_o$  or  $C_f$ ) values are reversed to polarization resistance. While the solution resistance ( $R_u$ ) decreases with the aging temperature increasing. And the values of reaction order ( $\alpha$ ) are about the same values which mean the surface of the samples was subjected to the same reactions state. Figure 4 shows EIS test results of solution heat treatment of AA2024 alloy that artificially aged at temperatures (150, 200, 250, and 300°C) with aging time 2 hours, and exposed to natural rainwater. From these curves the polarization resistance ( $R_p$ ) increases first up to 200°C aging temperature and then decreases, this is because of the precipitate coherency behavior for both ( $Al_2Cu$  and  $Al_2CuMg$ ) and seems less fluctuation than 1 hour aging time. The capacitors ( $Y_o$  or  $C_f$ ) values are reversed to polarization resistance. While the solution resistance ( $R_u$ ) had oscillated decrease, then increase and decrease with aging temperature, this behavior may be due to several types of corrosion occurring at the same time. And the values of reaction order ( $\alpha$ ) are about the same values which mean the surface of the samples was subjected to the same reactions state. Figure 5 shows EIS test results of solution heat treatment of AA6061 alloy that artificially aged at temperatures (150, 200, 250, and 300°C) with aging time 1 hour, and exposed to natural rainwater. From this figure, by comparing the resistances and capacitors, the polarization resistance ( $R_p$ ) varied increase and decrease with aging temperatures. This behavior is due to the intermetallic compound precipitation ( $Mg_2Si$ ) its size and distribution on the sample surface. The capacitors ( $Y_o$  or  $C_f$ ) values are reversed to polarization resistance. While the solution resistance ( $R_u$ ) behaviors are the same as polarization resistance. And the values of reaction order ( $\alpha$ ) are the same values except for aging at 200°C, which gave a 0.9 value which means the surface of the sample reaction is about uniform, while others were subjected to the same reaction state. Figure 6 shows EIS test results of solution heat treatment of AA6061 alloy that artificially aged at temperatures (150, 200, 250, and 300°C) with aging time 2 hours, and exposed to natural rainwater. From this figure, by comparing the resistances and capacitors, the polarization resistance ( $R_p$ ) at first increases and then decreases with aging temperatures. This behavior is due to the intermetallic compound precipitation ( $Mg_2Si$ ) its growth and distribution on the sample surface. The capacitors ( $Y_o$  or  $C_f$ ) values are fluctuating increasing and decreasing. While the solution resistance ( $R_u$ ) behaviors are reversed to capacitor values. The values of reaction order ( $\alpha$ ) are about the same values which mean the surface of the samples was subjected to the same reactions state.

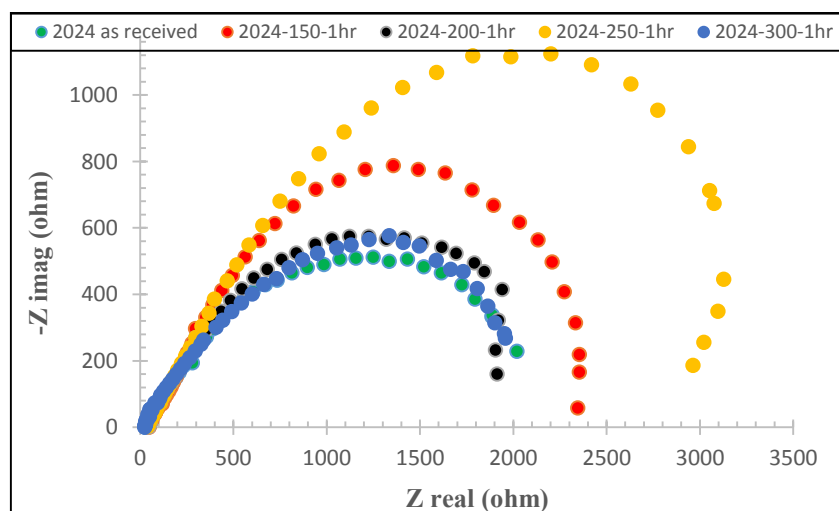


Figure 3. Nyquist plot of AA2024 after solution heat treatment and aging at temperatures (150, 200, 250, and 300°C) for 1hr in rainwater.

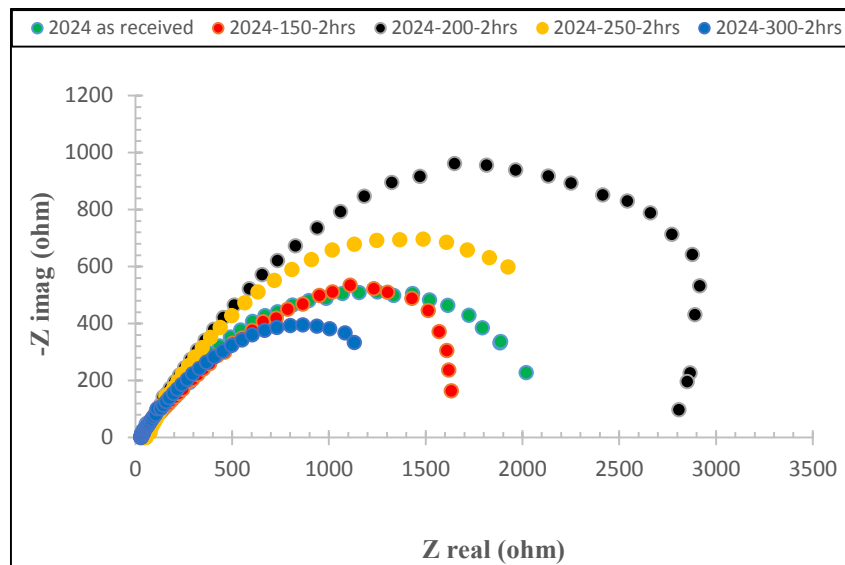


Figure 4. Nyquist plot of AA2024 after solution heat treatment and aging at temperatures (150, 200, 250, and 300 °C) for 2hr in rainwater.

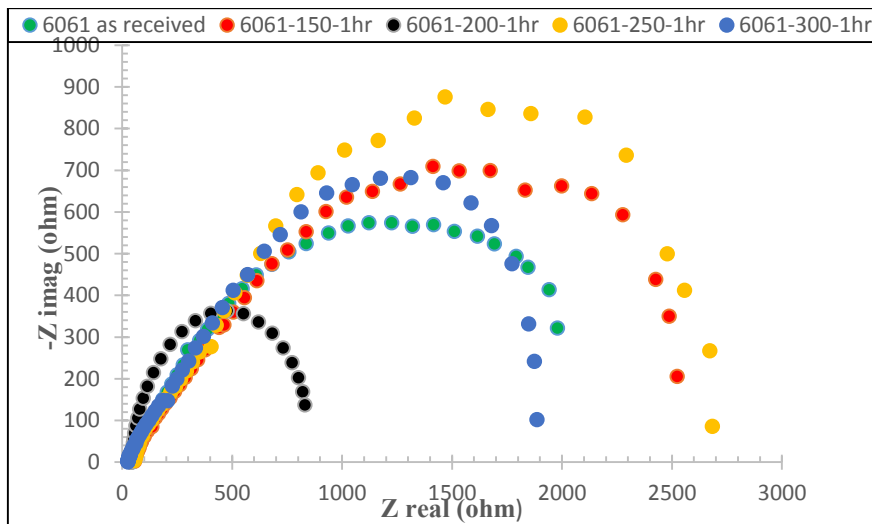


Figure 5. Nyquist plot of both AA6061 after solution heat treatment and aging at temperatures (150, 200, 250 and 300 °C) for 1hr in rainwater.

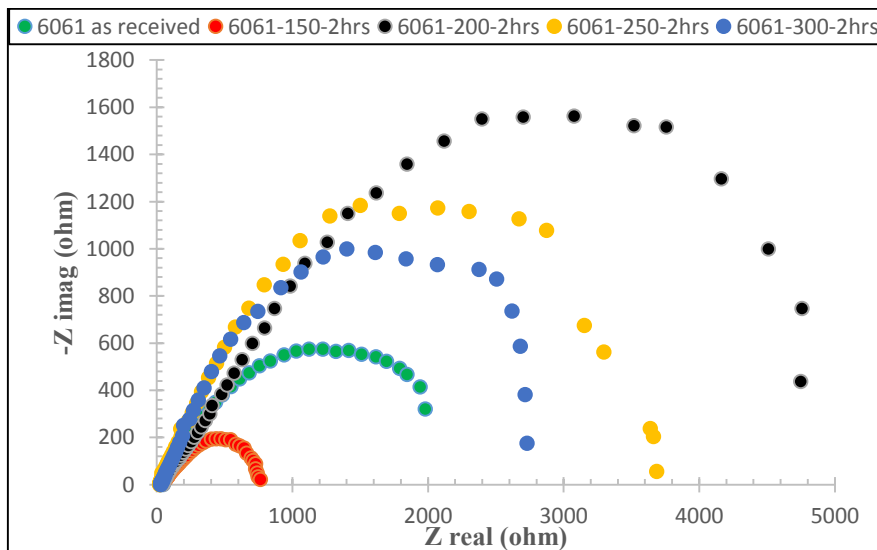


Figure 6. Nyquist plot of both AA6061 after solution heat treatment and aging at temperatures (150, 200, 250 and 300 °C) for 2hr in rainwater.

Table 4. The resistors and capacitors of AA2024 alloy after solution heat treatments in rainwater.

Alloys	Rp( ohms)	Ru(ohms)	Cf( $\mu$ F)	$\alpha$
2024,150 °C,1h	$2.919 \times 10^3$	45.66	75.23	0.584
2024,150 °C,2h	$1.993 \times 10^3$	37.72	135.0	0.542
2024,200 °C,1h	$2.263 \times 10^3$	41.76	80.53	0.586
2024,200 °C,2h	$3.408 \times 10^3$	34.22	40.38	0.598
2024,250 °C,1h	$4.033 \times 10^3$	37.79	58.65	0.572
2024,250 °C,2h	$2.802 \times 10^3$	51.92	176.8	0.594
2024,300 °C,1h	$2.296 \times 10^3$	18.40	86.81	0.541
2024,300 °C,2h	$1.556 \times 10^3$	26.93	288.0	0.570

Table 5. The resistors and capacitors of AA6061 alloy after solution heat treatments in rainwater.

alloys	Rp( ohms)	Ru( ohms)	Cf( $\mu$ F)	$\alpha$
6061,150 °C,1h	$2.932 \times 10^3$	47.95	73.64	0.552
6061,150 °C,2h	873.0	34.84	182.5	0.482
6061,200 °C,1h	847.3	40.94	175.2	0.901
6061,200 °C,2h	$6.937 \times 10^3$	39.93	80.19	0.529
6061,250 °C,1h	$3.292 \times 10^3$	48.01	67.25	0.582
6061,250 °C,2h	$4.090 \times 10^3$	20.78	66.57	0.674
6061,300 °C,1h	$2.582 \times 10^3$	21.60	152.1	0.559
6061,300 °C,2h	$3.346 \times 10^3$	26.91	69.49	0.648

Figure 7 and Table 6 show phases obtained from the XRD test. From these figures and table the maximum value for AA2024 of intensity was 100 at a position of  $2\theta = 44.68$  aging treatments at temperature 250°C for 2hrs. And for AA6061 the maximum value of intensity was 100 at a position  $2\theta = 44.68$  aging treatments at temperature 300°C for 1hr. After solution heat treatments of AA2024 alloy,  $Al_2Cu$  and  $Al_2CuMg$  precipitate phases are formed. While after solution heat treatments of AA6061 alloy, the  $Mg_2Si$  precipitate phase formed.

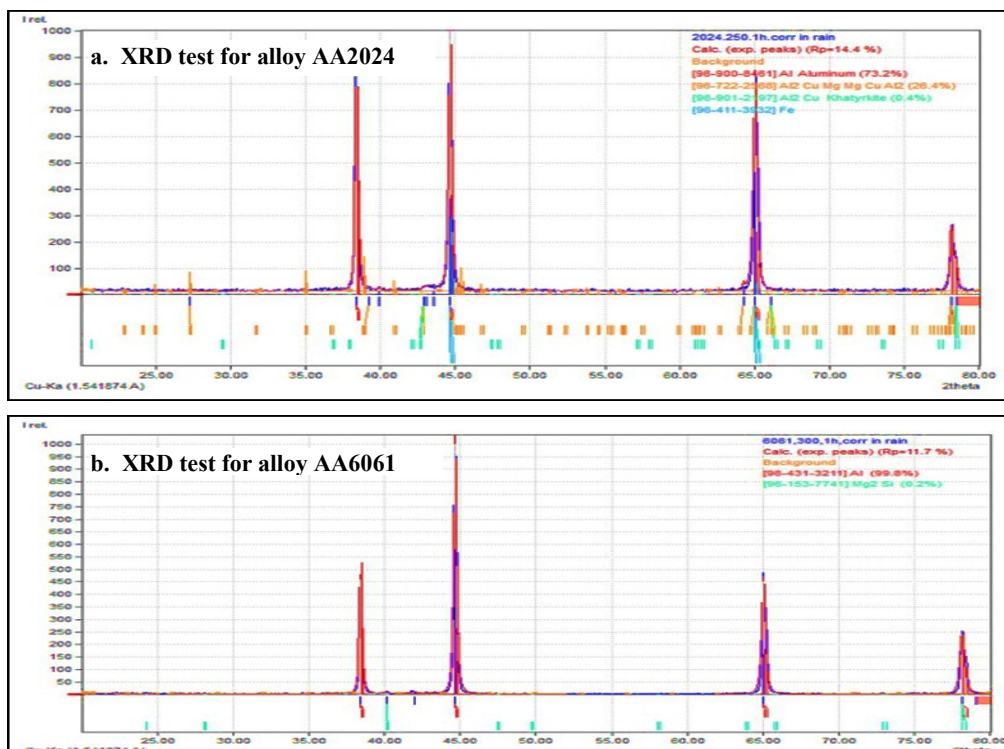
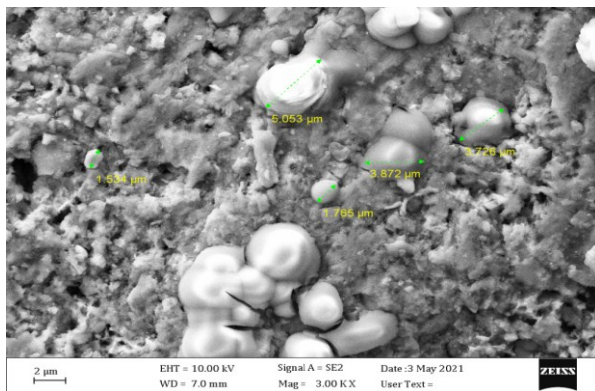


Figure 7. XRD inspection alloy (a) alloy AA2024 solution heat treatment and aging at temp.250 °C for 1hr. and (b) alloy AA6061 solution heat treatment and aging at temp.300 °C for 1hr.

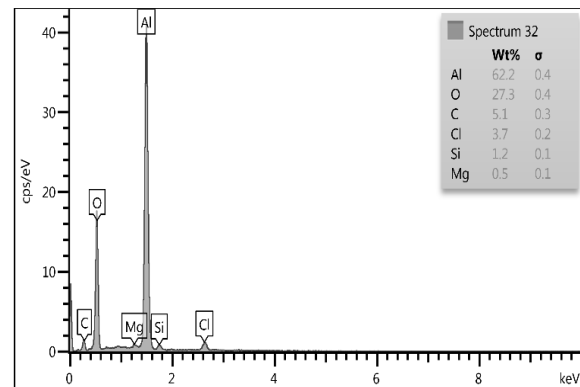
Table 6. Phases obtain from the XRD test.

Alloys	phase	2Theta	I/I1	Crystal system
AA2024 solution heat treatment and aging at temp.250 °C for 2hrs.	Al	38.43, 44.68, 65.04, 78.19, 78.44	81,100,97,29,97.65	Cubic
AA2024 solution heat treatment and aging at temp.250 °C for 2hrs.	Al <sub>2</sub> CuMg	27.24,39.24, 42.88,44.68, 64.28,65.04, 66.04, 78.19, 78.44	6.61, 9.49, 4.10,100, 26.51,6.96, 97, 29 ,6.96	Orthorhombic
AA2024 solution heat treatment and aging at temp.250 °C for 2hrs	Al <sub>2</sub> Cu	42.88, 65.04, 66.04, 78.44	4.10,97,6.96,6.96	Tetragonal
AA6061 solution heat treatment and aging at temp.300 °C for 1hr.	Al	38.44, 44.68, 65.04, 78.16,	44,100,53,30	Cubic
AA6061 solution heat treatment and aging at temp.300 oC for 1hr.	Mg <sub>2</sub> Si	40.12, 78.16	5.22,30	Cubic

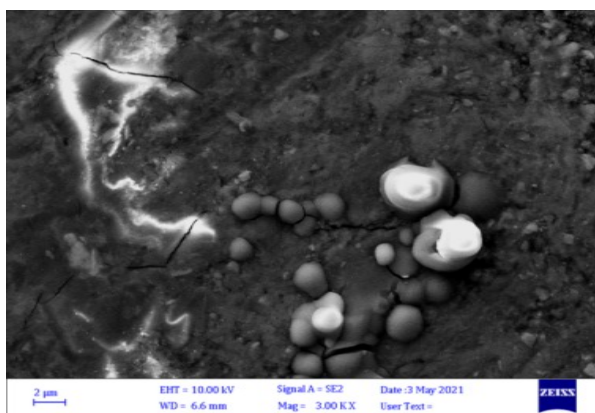
Figure 8 shows SEM and EDS test results of AA2024 and AA6061 after solution heat treatment. From these tests, it is found that the change in the values of the resistors and capacitors in the EIS test is affected by the precipitated phases due to the solution treatment, as well as the formation of oxide and chloride layers as corrosion products due to rainwater environment.



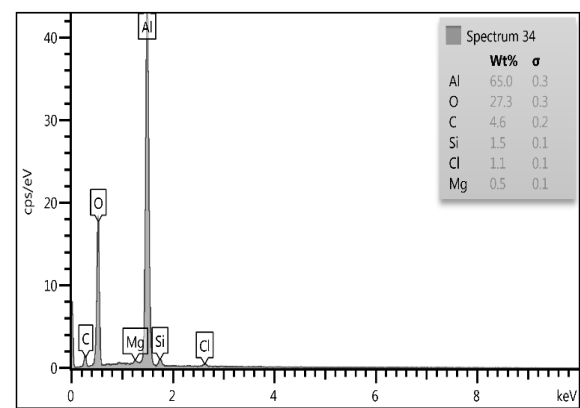
a. SEM test of AA2024, , 3000X



b. EDS test of AA2024



c. SEM test of AA6061, 3000X



d. EDS test of AA6061

Figure 8. SEM and EDS test for (a) and (b) for alloy AA2024 solution heat treatment and aging at temp.250 °C for 1hr. (c) and (d) for alloy AA6061 solution heat treatment and aging at temp. 300 °C for 1hr.

#### 4. Conclusions

- 1- The EIS test of as received AA2024 alloy, indicate that the polarization resistance ( $R_p$ ) and capacitance ( $C_f$ ) values are higher than for as receiving AA6061 alloy, which clarifies that the corrosion resistance of AA2024 is lower than AA6061 in rainwater.
- 2- The behavior of Nyquist curves of AA2024 after solution heat treatment and aging at temperatures (150, 200, 250, and 300°C) for 1hr and exposed to natural rainwater, shows fluctuation values of the polarization resistance ( $R_p$ ) and capacitance ( $C_f$ ), which indicate that the reaction of alloy surface non-uniform, because of the precipitate particles are random dispersion on the surface. While the polarization resistance ( $R_p$ ) and capacitance ( $C_f$ ) of 2 hours aging show fewer variations in their values, and towards uniformity. These behaviors are the same for alloy AA6061 solution heat treatment and aging same temperatures and for the same times.
- 3- The XRD test shows that the precipitation phases for AA2024 alloy after solution heat treatment and aging are ( $Al_2Cu$  and  $Al_2CuMg$ ). While the precipitation phase for AA6061 alloy is ( $Mg_2Si$ ). These precipitate particles, does not uniform in their sizes and distributions on the sample surfaces, which they responsible for the non-uniform reaction. And may the cause micro galvanic cells.
- 4- The constitutes of the composition of natural rain rainwater salinity, have a great effect on the interactions that occur on the surface of the alloys, and they certainly have an effect on the solution resistance ( $R_u$ ) values recorded in the EIS test, they seem to be reverse to polarization resistance.
- 5- The compatibility type of EIS tests was Constant Phase Element (CPE) fitting model due to the formation of a layer of corrosion products which behaves like a coating layer.

#### Acknowledgments

The authors would like to express their gratitude to the personnel of Mustansiriyah University in Baghdad, Iraq ([www.upomustansiriyah.edu.iq](http://www.upomustansiriyah.edu.iq)) for their assistance with this project.

#### References

- [1] Gilbert Kaufman J. (2000), "Introduction to Aluminum Alloys and Tempers", ASM International.
- [2] Milkereit, B. , Kessler, O. , and Schick, C. Recording of continuous cooling precipitation diagrams of aluminum alloys, *Thermochimica Acta*, Volume 492 (2009) pp. 73-78 .
- [3] Davis J. R., (1993), *Aluminum and Aluminum Alloys*, in ASM Specially Handbook, ASM, International, Metal Park, Ohio.
- [4] Callister, W. D., (1997), *Material Science and Engineering*, John Wiley and Sons, New York.
- [5] Takahashi, A., Mori, E., and Ohnishi, T. The foci of DNA double strand break-recognition proteins localize with  $\gamma$ H2AX after heat treatment, *Journal of radiation research*, Vol. 51 (2010) pp. 91-95
- [6] ASM International Subject Guide (2015), Materials Park, Ohio.
- [7] Avner, Sidney H., (1982), *Introduction to Physical Metallurgy*, McGraw-Hill International Book Company, Tokyo.
- [8] Abubakre O. K., Mamaki U.P. And Muriana R. A (2009), "Investigation of the Quenching Properties of Selected Media on 6061 Aluminum Alloy", *Journal of Minerals & Materials Characterization & Engineering*, Vol. 8, No.4, pp 303-315,USA.
- [9] Pohlman S. L., in ASM Handbook, Volume 13, Corrosion, edited by J. R. Davis. ASM International, Materials Parks, OH, 1987, pp. 80-103.
- [10] "Corrosion of Aluminum and Aluminum alloys", ASM International, 1999.
- [11] Chen, Y.Q.; Pan, S.P.; Zhou, M.Z.; Yi, D.Q.; Xu, D.Z.; Xu, Y.F. Effects of inclusions, grain boundaries and grain orientations on the fatigue crack initiation and propagation behavior of 2524-T3 Al alloy. *Mater. Sci. Eng. A* 2013, 580, 150-158 .
- [12] Golden, P. A comparison of fatigue crack formation at holes in 2024-T3 and 2524-T3 aluminum alloy specimens. *Int. J. Fatigue* 211-219,21,1999.
- [13] JOGI, B. F.; BRAHMANKAR, P. K.; NANDA, V. S.; PRASAD, R. C. Some studies on fatigue crack growth rate of aluminum alloy 6061. *Journal of Materials Processing Technology*, v. 201, p. 380-384, 2008.
- [14] ADESOLA, A. O.; ODESHI, A. G.; LANKE, U. D. The effects of aging treatment and strain rates on damage evolution in AA 6061 aluminum alloy in compression. *Materials and Design*, v. 45, p. 212-221, 2013.
- [15] DEMIR, H.; GÜNDÜZ, S. The effects of aging on machinability of 6061 aluminum alloy. *Materials and Design*, v. 30, p. 1480-1483, 2009.
- [16] TROEGER, L. P.; STARKE, E. A. Microstructural and mechanical characterization of a superplastic 6XXX alloy. *Materials Science and Engineering A*, v. 277, p. 102-113, 2000.
- [17] Ghali E., in *Uhlig's Corrosion Handbook*, 2nd edition, edited by R. W. Revie. Wiley, Hoboken, NJ, 2000, pp. 677-715
- [18] "Basics of Electrochemical Impedance Spectroscopy," Application Note Rev. 1.0 11/9/2016 © Copyright 1990-2016 Gamry Instruments, Inc. pp 1-19.
- [19] Association, A. International alloy designations and chemical composition limits for wrought aluminum and wrought aluminum alloys. *Teal Sheets 2009* cited Access 2009 accessed: 22/7/2020; 1-28 Available from: <https://www.aluminum.org/sites/default/files/Teal%20Sheet.pdf>